Surfactant-mediated epitaxy of metastable SnGe alloys

P. F. Lyman and M. J. Bedzyk

Materials Research Center and Department of Materials Science and Engineering, Northwestern University, Evanston, Illinois 60208 and Materials Science Division, Argonne National Laboratory, Argonne, Illinois 60439

An effective method for molecular beam epitaxial construction of metastable, pseudomorphic SnGe/Ge(001) heterostructures is presented. This method exploits a surfactant species, Bi, to alter Sn surface-segregation kinetics. Using the x-ray standing wave technique, we demonstrate not only that Bi segregates to the growth surface more strongly than Sn, but that it also dramatically suppresses the segregation mobility of Sn. The limited Sn diffusivity, which is believed to stem from the full coordination of subsurface Sn atoms, allows the epitaxy of well-ordered, metastable SnGe heterostructures. © *1996 American Institute of Physics.* [S0003-6951(96)05133-9]

Alloys and short-period superlattices of Sn and Ge are predicted to possess a direct and tunable band gap for certain stoichiometries and superlattice structures.[1–5] Moreover, due to small effective masses and a lack of polar scattering (inherent in III–V compounds), carrier mobilities are expected to be high.[1,6] The predicted band gap would make Sn_xGe_{1-x} suitable for long-wavelength photodetectors and emitters, opening the possibility of constructing tunable, infrared optoactive devices based on the inexpensive and well-developed technologies of group IV semiconductors. Unfortunately, serious impediments hinder SnGe alloy production. The lattice mismatch between α-Sn and Ge is large ($\sim$15%), and bulk α-Sn transforms to β-Sn at 13.2 °C. Heteroepitaxial stabilization of α-Sn films on lattice-matched substrates, however, can raise the α–β transition temperature to >100 °C.[7,8] Perhaps the most serious difficulty to be overcome is the low solid solubilities of Sn in Ge and Ge in Sn, which are <1%.[9] In molecular beam epitaxial (MBE) growth of SnGe, this incompatibility results in rapid Sn segregation.[10]

The presence of a surfactant species on the growth surface during MBE (surfactant-mediated epitaxy, or SME) profoundly alters the kinetics of important surface processes, such as adatom diffusion[11] and island nucleation,[12] which can change the film's growth morphology.[11,12] Also, SME allows the construction of abrupt interfaces where segregation of the substrate material ordinarily leads to interface smearing. For example, when Si is deposited on bare Ge, the lower surface energy of Ge drives its segregation into the Si. A surfactant, however, fully coordinates the outermost Ge atoms; this raises the energy barrier for Ge exchange, inhibiting Ge segregation.[12] We will show that a surfactant also suppresses segregation in SnGe; although there is a higher driving force for Sn segregation, the kinetic barrier posed by the surfactant greatly suppresses it.

SME growth of Ge/Sn/Ge(001) must proceed in two stages: deposition of Sn on the surfactant-covered Ge surface, and subsequent Ge growth. The requirements for an effective surfactant for SnGe growth are: (1) it must segregate during Sn deposition, and (2) it must prevent Sn segregation during Ge growth (as for Si/Ge). This letter reports a study of the segregation and structural perfection of Bi, Sn, and Ge on Ge(001) using the x-ray standing wave (XSW)

technique, Auger electron spectroscopy (AES), and low energy electron diffraction (LEED). We demonstrate that Bi meets these criteria, and show that crystalline Ge/Sn/Ge(001) pseudomorphic structures may be formed by SME.

The experiments were conducted at beamline X15A of the National Synchrotron Light Source in an ultrahigh vacuum chamber ($P_{base}<10^{-10}$ Torr) that allows LEED, AES, and XSW measurements (see Ref. 13). After Ne$^+$ ion sputtering (500 eV at 500 °C) and annealing (690 °C), all growth commenced on clean Ge(001) surfaces exhibiting a (2×1) LEED pattern with $c(2\times4)$ streaks. Pure Bi, Sn, and Ge were deposited from BN effusion cells at rates of 2, 0.5, and 4 ML/min, respectively. Rates were calibrated using a quartz-crystal oscillator; coverages were achieved by timed depositions and verified by AES. The pressure remained $<10^{-9}$ Torr during Ge deposition and $<3\times10^{-10}$ Torr for Sn and Bi growth.

In the XSW method,[13] a monochromatic x-ray beam is Bragg-reflected from a single crystal sample. The interference of the incident and reflected plane waves generates an XSW in and above the crystal; the XSW nodal planes are parallel to, and have the same periodicity as, the diffraction planes. The phase v of the outgoing wave with respect to the incident wave shifts by 180° as the Bragg angle θ is scanned upwards from the low-angle side of the rocking curve, causing the antinodal planes of the XSW to move inward by one-half of the d-spacing d_{hkl}. The resultant modulation of the fluorescence yield Y from an adatom layer is given by $Y(\theta)=1+R(\theta)+2\sqrt{R(\theta)}f_H\cos[v(\theta)-2\pi P_H]$, where the parameters f_H (coherent fraction) and P_H (coherent position) also correspond to the amplitude and phase, respectively, of the Hth Fourier component of the spatial distribution of the adatoms' nuclei (projected into a unit cell). [$\mathbf{H}\leftrightarrow(hkl)$.] For a surface experiment, P_H is the adsorption height (in units of d_{hkl}) of the atom under study relative to the outermost bulk-like lattice plane. Note that a "modulo-d ambiguity" allows only the position of the layer with respect to a bulk plane to be determined.

To establish that Bi segregates upon Sn deposition, we used AES and also monitored the Bi adsorption height using XSW. After Bi deposition on Ge(001) at $T_{sub}\approx400$ °C, the LEED pattern was $(2\times n)$, $n\approx8$, similar to Bi/Si(001).[14] The saturation Bi coverage is presumably $(n-1)/n$, $\approx7/8$
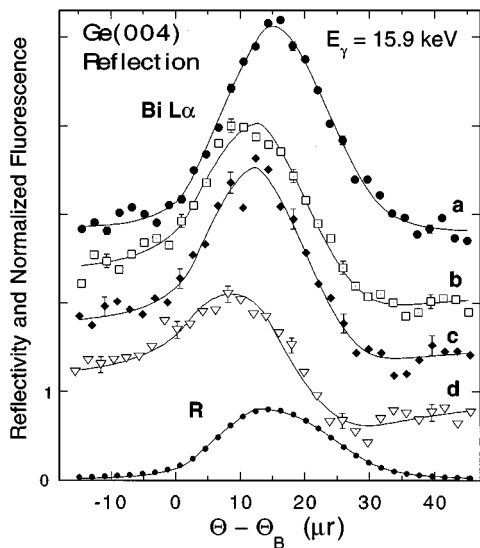
FIG. 1. Ge(004) reflectivity and Bi XSW analysis of: (a) Bi/Ge(001) ($P_{004}^{Bi}=1.28\pm0.01$, $f_{004}=0.93\pm0.05$); (b) Bi/0.6 ML Sn/Ge(001) ($P_{004}^{Bi}=1.41\pm0.01$, $f_{004}=0.76\pm0.04$); (c) Bi/40 ML Ge/0.6 ML Sn/Ge(001) ($P_{004}^{Bi}=1.40\pm0.01$, $f_{004}=0.81\pm0.05$); (d) Bi/2 ML Sn/Ge(001) ($P_{004}^{Bi}=1.55\pm0.01$, $f_{004}=0.70\pm0.04$). The line through the reflectivity is a fit (Ref. 13) to dynamical diffraction theory, and the lines through the modulated fluorescent yield are fits using the equation in the text. [Lines (a) through (c) are offset for clarity.]

ML, at this temperature (1 ML$= 6.25\times10^{14}$ cm^{-2}). The Bi adsorption position was then determined using XSW. Next, the substrate was heated to $\approx$300 °C, and $\approx$0.6 ML Sn was deposited. The LEED pattern weakened slightly; the Bi AES intensity did not decrease, consistent with Bi segregation. Bi XSW analysis was repeated. Next, $\sim$40 ML of Ge was deposited at $T_{sub}\approx$300 °C. Again, the LEED pattern remained ($2\times n$); the only change seen by AES was a marked decrease in Sn intensity. Finally, Bi XSW analysis was repeated. This procedure was repeated for $\approx$2.0 ML of Sn deposition on Bi/Ge(001). (Ge deposition was not carried out.)

Bi XSW results are shown in Fig. 1. The Bi yield curves change with Sn coverage. This is consistent with the Bi adsorption height increasing upon Sn deposition. On the Bi/Ge(001) surface (without Sn), $P_{004}^{Bi}=1.28\pm0.01$ [Fig. 1(a)]; thus, the Bi adsorption height is $h_{Bi}=d_{004}$ $P_{004}^{Bi}=1.81$ Å. Since Sn is larger than the host Ge atoms, the average Bi position (relative to the diffraction planes) will increase upon Sn deposition if Sn and Bi exchange places, rendering Bi/Sn/Ge(001). For 0.6 ML of Sn, P_{004}^{Bi} was 1.41 ± 0.01 [Fig. 1(b)]. For 2.0 ML of Sn, $P_{004}^{Bi}=1.55\pm0.01$ [Fig. 1(d)]. The increase in Bi position with Sn coverage indicates Bi segregation. Interestingly, deposition of $\sim$40 ML of Ge on the Bi/0.6 ML Sn/Ge(001) structure had no effect on the Bi position [Fig. 1(c)]. However, if Bi segregates, its position relative to the diffraction planes would remain the same, since the deposited Ge film will have the substrate lattice spacing. Conversely, the Bi position would likely be altered if it were covered by Ge. Clearly, Bi segregates during growth of either Sn or Ge.

The second criterion for SME of SnGe is the inhibition of Sn segregation during Ge overgrowth. We analyzed Ge/
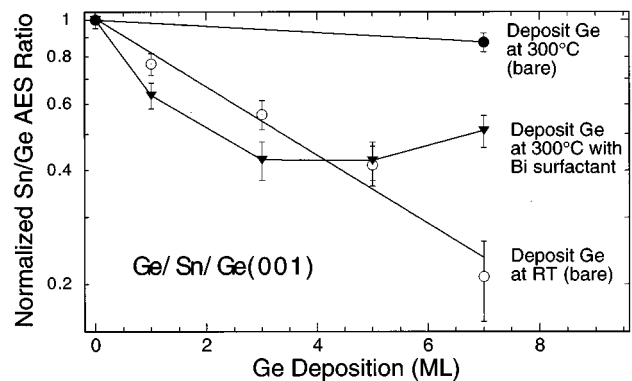
FIG. 2. Normalized Sn/Ge AES ratio vs Ge deposition on $\approx$0.6 ML Sn/Ge(001). Straight lines are fits to an exponential; the line for Bi data is a guide to the eye.

Sn/Ge(001) growth by AES for several conditions. For all, we deposited $\approx$0.6 ML of Sn on a Ge(001) substrate, and subsequently grew $\approx$7 ML of Ge (periodically interrupted for AES analysis). For a bare substrate (no surfactant), Ge deposition at room temperature reduced the (Sn MNN)/(Ge LMM) AES ratio in a nearly exponential fashion (Fig. 2); this is the signature of the burial of Sn by Ge, i.e., no Sn segregation. In contrast, when this was repeated at $T_{sub}=$300 °C, almost no decrease in the Sn/Ge ratio resulted, consistent with strong Sn segregation. Finally, this was repeated for Bi/Ge(001) at $T_{sub}=$300 °C. For Ge depositions $<$4 ML, a dramatic decrease in the Sn/Ge AES ratio was observed, consistent with effective Sn burial. However, the Sn signal saturated at a nearly constant value above this Ge coverage; this is consistent with some of the Sn forming two-dimensional (2D) islands that lack a Bi overlayer, and thus are able to segregate. While the root of this small remaining segregation is unresolved, it is clear that Bi can profoundly suppress Sn segregation. Future work will focus on optimizing growth parameters and eliminating the small remaining Sn segregation.

Although these data show that Bi can suppress Sn segregation, they do not probe the crystalline perfection of the buried Sn. For that, we conducted an XSW analysis of the Sn layers in the Bi/Sn/Ge(001) and Bi/Ge/Sn/Ge(001) structures. For $\approx$0.6 ML of Sn deposited on Bi/Ge(001) at $T_{sub}=$300 °C, the data [Fig. 3(a)] reveal $P_{004}^{Sn}=1.12\pm0.01$, with $f_{004}=0.72\pm0.04$. Since some of this apparent disorder is from vibrational smearing of the Sn positions (Debye–Waller factor, $\approx$0.85[15]), this near-surface Sn must be fairly well ordered ($>$84%). After $\sim$20 ML of subsequent Ge deposition at $T_{sub}=$300 °C, P_{004}^{Sn} decreased slightly to 1.09 $\pm$0.01, while f_{004} was essentially constant at 0.69 ± 0.04 [Fig. 3(b)].

These adsorption positions P_{004}^{Sn} are consistent with a pseudomorphic, tetrahedrally coordinated Sn layer whose in-plane lattice constants are coherent with the Ge(001) substrate. For Bi/Sn/Ge(001), the near-surface, epitaxial 2D Sn islands may expand normal to the surface to compensate for the local in-plane strain. For Bi/Ge/Sn/Ge(001), long-range elastic forces imposed by the thick Ge overlayer dictate that the strain cannot be relieved *locally*, but that the average strain of the Sn layer instead results in a displacement of the
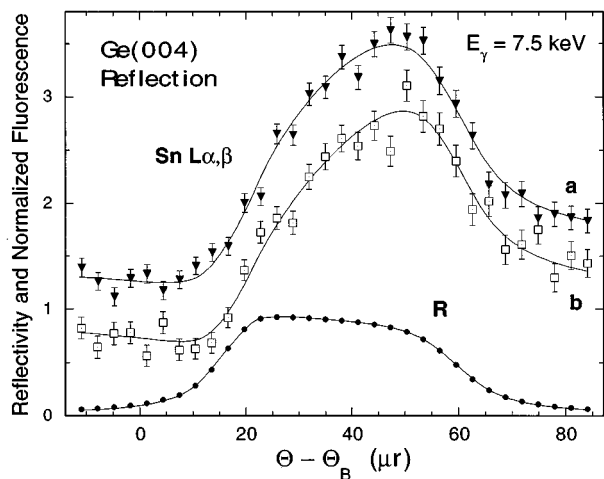
FIG. 3. Ge(004) reflectivity and Sn XSW results: (a) Bi/0.6 ML Sn/Ge(001) ($P_{004}^{Sn}=1.12\pm0.01$, $f_{004}=0.72\pm0.04$); (b) Bi/20 ML Ge/0.6 ML Sn/Ge(001) ($P_{004}^{Sn}=1.09\pm0.01$, $f_{004}=0.69\pm0.04$).

SnGe heterostructure. Thus, P_{004}^{Sn} is a function of Sn coverage, even for submonolayer growth. We calculated the expected displacement for one ML of Sn_xGe_{1-x} using both continuum elasticity theory and by a Keating calculation[16] (using Vegard's law in both for the elastic and lattice constants). These approaches yielded indistinguishable predictions. On the extremes, an isolated Sn atom would be characterized by $P_{004}^{Sn}=0$, while a uniform ML of Sn would attain $P_{004}^{Sn}\approx1.13$. Excellent agreement was found for our buried layer of 0.6 ML of Sn ($P_{exp}=1.09\pm0.01$, $P_{calc}=1.08$). Such calculations are not valid for surface species, but notice that the experimental Bi/0.6 ML Sn/Ge(001) result ($P_{004}^{Sn}=1.12\pm0.01$) matched well the Ge/1 ML Sn/Ge(001) calculations ($P_{calc}=1.13$). It seems reasonable that a 2D Sn island with a tetrahedral Bi termination would locally mimic a full Sn ML with a Ge cap.

There have been several previous attempts to construct crystalline, metastable SnGe alloys[10,17–20] and short-period superlattices[21] by imposing kinetic barriers to segregation and phase separation. The two most successful attempts[10,21] centered on introducing Sn atoms to subsurface sites via nonequilibrium routes; subsequent thermal diffusion to the surface (i.e., segregation) was suppressed by the high activation barrier to bulklike diffusion. Since Sn cannot segregate at low temperatures, Wegscheider and co-workers used thermal cycling to create short-period superlattices.[21] Sn and several Ge layers were deposited at $T_{sub}\leq100\,°C$, then T_{sub} was ramped to ~300 °C during continued Ge growth. Deposition was halted and the substrate cooled before the next Sn deposition. Using laborious thermal control, Sn_nGe_m structures ($n\leq2$, $m\geq9$) could be constructed. In a different approach, Atwater et al. created random Sn_xGe_{1-x} alloys ($x\sim0.3$) by nonthermally enhancing Sn incorporation with low-energy ion bombardment. Sn and Ge were deposited along with a flux of ~50 eV Ar$^+$ ions, causing shallow implantation of

Sn into the Ge substrate.[20] Although the growth temperature was elevated for epitaxial ordering, the full coordination of the subsurface Sn atoms retarded segregation,[20] again, by requiring bulklike diffusion.

SME of SnGe is similar: the surfactant adlayer strongly favors the transport of deposited Sn (or Ge) atoms to subsurface sites. After subsequent Ge deposition, the (now fully coordinated) Sn atoms would be required to break several bonds in order to segregate, thereby mimicking bulk diffusion. The sizable energy barrier to this process traps the Sn in metastable sites below the Ge. SME could realize a significant advantage for production of superlattices compared to strictly thermal control, as it requires neither awkward thermal cycling nor growth at suboptimal temperatures. Moreover, SME could be used for production not only of superlattices *but also* of random alloys by proper choice of the Sn and Ge fluxes; neither thermal cycling nor ion-assisted growth has the potential to produce both types of heterostructures.

[1] D. W. Jenkins and J. D. Dow, Phys. Rev. B **36**, 7994 (1987).
[2] K. A. Mäder, A. Baldereschi, and H. von Känel, Solid State Commun. **69**, 1123 (1989).
[3] J. Olajos, P. Vogl, W. Wegscheider, and G. Abstreiter, Phys. Rev. Lett. **67**, 3164 (1991).
[4] T. Brudevoll, D. S. Citrin, N. E. Christensen, and M. Cardona, Phys. Rev. B **48**, 17128 (1993).
[5] D. Munzar and N. E. Christensen, Phys. Rev. B **49**, 11238 (1994).
[6] C. H. L. Goodman, IEEE Proc. I **129**, 189 (1982).
[7] J. L. Reno and L. L. Stephenson, Appl. Phys. Lett. **54**, 2207 (1989).
[8] M. T. Asom, A. R. Kortan, L. C. Kimerling, and R. C. Farrow, Appl. Phys. Lett. **55**, 1439 (1989).
[9] C. D. Thurmond, F. A. Trumbore, and M. Kowalchik, J. Chem. Phys. **24**, 799 (1956); C. D. Thurmond, J. Phys. Chem. **57**, 827 (1953).
[10] P. R. Pukite, A. Harwit, and S. S. Iyer, Appl. Phys. Lett. **54**, 2142 (1989).
[11] B. Voigtländer, A. Zinner, T. Weber, and H. P. Bonzel, Phys. Rev. B **51**, 7583 (1995).
[12] M. Copel, M. C. Reuter, M. Horn von Hoegen, and R. M. Tromp, Phys. Rev. B **42**, 11682 (1990).
[13] J. Zegenhagen, Surf. Sci. Rep. **18**, 199 (1993).
[14] T. Hanada and M. Kawai, Surf. Sci. **242**, 137 (1991); the $(2\times n)$ pattern arises from a dimerized, (2×1)-like local structure with every nth Bi dimer missing.
[15] P. F. Lyman, Y. Qian, T.-L. Lee, and M. J. Bedzyk, Physica B **221**, 426 (1996).
[16] P. N. Keating, Phys. Rev. **145**, 637 (1966).
[17] S. I. Shah, J. E. Greene, L. L. Abels, Qi Yao, and P. M. Raccah, J. Cryst. Growth **83**, 3 (1987).
[18] H. Höchst, M. A. Engelhardt, and I. Hernández-Calderón, Phys. Rev. B **40**, 9703 (1989).
[19] H.-J. Gossmann, J. Appl. Phys. **68**, 2791 (1990).
[20] G. He and H. A. Atwater, Nucl. Instrum. Methods B **106**, 126 (1995).
[21] W. Wegscheider, K. Eberl, U. Menczigar, and G. Abstreiter, Appl. Phys. Lett. **57**, 875 (1990).